FEATURE ARTICLE

Enantioselective Quenching of Luminescence: Molecular Recognition of Chiral Lanthanide Complexes by Biomolecules in Solution

Stefan C. J. Meskers* and Harry P. J. M. Dekkers*

Eindhoven University of Technology, Laboratory of Macromolecular and Organic Chemistry, P.O. Box 513, NL-5600 MB Eindhoven, The Netherlands

Received: December 7, 2000; In Final Form: February 26, 2001

Principles, experimental techniques, and applications of enantioselective quenching of lanthanide luminescence are addressed. Upon the addition of chiral, enantiomerically resolved quencher molecules to an aqueous, racemic solution of the tris (pyridine-2,6-dicarboxylate) chelate of Eu(III) or Tb(III), strong quenching of the lanthanide luminescence is observed, with a quenching rate that depends on the chirality of the lanthanide species. Quenching by *c*-type cytochromes and vitamin B_{12} derivatives is discussed in detail. For the latter quenchers, the energy transfer reaction held responsible for the quenching proceeds via formation of an encounter complex between donor and quencher in which the actual energy transfer takes place. A structural model for this transient pair has been constructed on the basis of data on complexation between B_{12} and ground-state lanthanide chelate obtained by measurements of lanthanide induced shifts and relaxation of the NMR signals of protons of B_{12} and from the induced circular dichroism spectra. The enantioselectivity in the quenching results mainly from selective binding of the two lanthanide enantiomers to B_{12}. A smaller contribution to the selectivity comes from differences in the rate of the quantum mechanical energy transfer within the two diastereomeric encounter complexes. Finally, the use of the enantiodifferential quenching to study complexation of B_{12} with two B_{12} binding proteins (haptocorrin and a monoclonal antibody) is addressed.

Introduction

About a decade ago it was discovered that pronounced chiral discrimination occurs in the quenching of the luminescence of a chiral racemic donor by a chiral, enantiomerically resolved quencher.[1,2] The quencher molecule preferentially accepts energy from one enantiomeric form of the donor and is less reactive toward the other mirror image related form. The electronic energy transfer reaction, which takes place in solution, provides a simple and convenient model system to study chiral discrimination, a general phenomenon which plays an important role in many (bio)chemical reactions.

If the enantiomers of the (excited) donor are denoted by Λ* and Δ* and those of the acceptor by r and s, four different pairs are possible for these chiral reaction partners: Λ*−r, Δ*−r, Λ*−s, and Δ*−r. On the basis of symmetry arguments, the rates of energy transfer for the Λ*−r and Δ*−s pairs are identical. The same holds for the Λ*−s and Δ*−r combination. The Λ*−r and Δ*−r pairs have a diastereomeric relation, and hence, the associated rates may be different. This is then referred to as enantioselectivity displayed by the quencher

$$\Lambda^* + r \rightarrow [\Lambda^* r]^{\ddagger} \rightarrow \Lambda + r^*$$

$$\Delta^* + r \rightarrow [\Delta^* r]^{\ddagger} \rightarrow \Delta + r^*$$

We assume that the energy transfer proceeds via a transition state in which donor and acceptor are in proximity (as a result of diffusional motion). The higher reactivity of one enantiomer over its mirror image of equal energy and stability is obviously due to differences in the enthalpy and entropy of activation associated with the two diastereomeric transition states. A second contribution to the chiral discrimination stems from differences in the quantum mechanical matrix element describing the electronic coupling between donor and acceptor in the two transition states.

Particularly well-studied are the energy transfer reactions involving the chiral lanthanide complexes $Eu(dpa)_3^{3-}$ and $Tb(dpa)_3^{3-}$ as the energy donor (dpa denotes pyridine-2,6-dicarboxylate dianion, see Figure 1). These complexes are chemically stable, strongly luminescent with excited-state lifetimes in the order of milliseconds, and exhibit large values of circular polarization in their luminescence (CPL). A large variety of chiral molecules was found to discriminate between the two enantiomers of the lanthanide chelate when acting as acceptor; small inorganic compounds (e.g., cobalt hexamine chelates,[3−11] $Ru(phen)_3^{3-}$ [12−18]), organic dye molecules[19] (urobilin derivatives), molecules with topological chirality[20] (a dinuclear copper(I) knot), transition metal−nucleotide complexes,[21,22] metalloproteins (*c*-type cytochromes[23−25] blue copper proteins,[26] myoglobin, and hemoglobin[27]), vitamin B_{12} derivatives,[28] and, finally, vitamin B_{12}−protein complexes.[29] Therefore, it might be said that enantioselectivity in energy transfer reactions involving lanthanide chelates is quite a general phenomenon. An interesting question is whether and how the

* Corresponding authors. Tel: +31-(0)40-2473109. Fax +31-(0)40-2451036. E-mail: s.c.j.meskers@tue.nl.

10.1021/jp004428w CCC: $20.00
Published on Web 04/20/2001

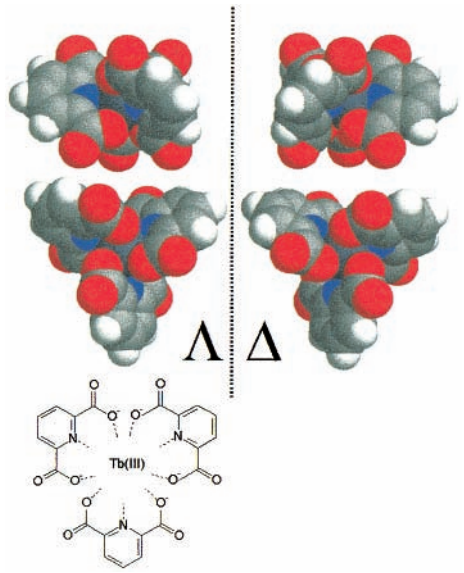

Figure 1. Structure of the $Ln(dpa)_3^{3-}$ chelates. The enantiomer with right (left) handed helicity around the 3-fold symmetry axis is labeled by Δ (Λ).

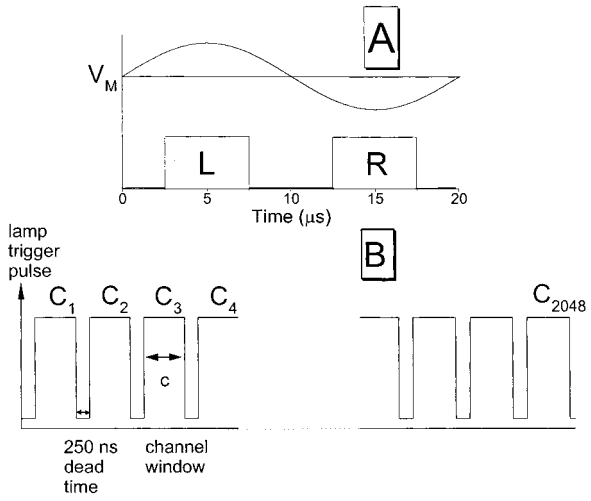

Figure 2. Schematic diagram of the electronic signal processing in the CPL measurement. The part A shows the sinoidal driving voltage V_M of the photoeleastic modulator (50 kHz) and the electronic gates for the photopulses. The L and R gates correspond to Left and Right circular polarization detection. The lower part B shows the time channels involved in time-resolved measurements; the dead time between the channels is 250 ns.

chiral discrimination in the transfer can be related to molecular structure. This question is the major topic of this review. First, we will discuss the experimental procedures used to determine the enantioselectivities and then review studies on series of related metalloproteins which reveal that the molecular (surface) structure is indeed important in determining the enantioselectivity. Subsequently, focusing on the transfer reactions involving vitamin B_{12} derivatives, we will go one step further in analyzing the effect of molecular structure and distinguish between the contribution from the differential stability of the $[\Lambda^*r]^‡$ and $[\Delta^*r]^‡$ activated donor−acceptor complexes to the overall enantioselectivity and the contribution due to the difference in energy transfer rates within these species.

Measurement of Circularly Polarized Luminescence

Chiral molecules absorb left and right circularly polarized light to a different extent (circular dichroism, CD), and their spontaneous emission has different probabilities for R and L light: their luminescence is circularly polarized (CPL).[30] The circular dichroism is characterized by the difference of the extinction coefficients for L and R light (cf eq 1). CPL is conveniently characterized by the degree of circular polarization of the luminescence, or dissymmetry factor, g_{lum} (see eq 2). Both CD and CPL are wavelength-dependent

$$\Delta\epsilon = \epsilon_L - \epsilon_R \tag{1}$$

$$g_{lum} = 2(I_L - I_R)/(I_L + I_R) \tag{2}$$

The excitation light source of our time-resolved CPL spectrometer[31] consists of a xenon flash lamp with variable pulse width and repetition rate. Wavelength selection is performed with a monochromator and/or optical filters. The circular polarization of the luminescence light from the sample is analyzed by a photoelastic modulator (M), operating at ∼50 kHz.[32] In the emission line, M is followed by a monochromator and a photomultiplier tube (PMT). The photo pulses from PMT are routed through a pulse height discriminator and a pulse shaper before entering the custum designed differential photon counter DPC. This instrument basically consists of two multichannel counters (the up-counter C+ and the down-counter C-, each coupled to a memory) and two timing devices. The first timer defines the central parts of the modulation half-cycles L and R, where modulation depth is optimal (see Figure 2). The second timer defines the positions of the decay channels C_i (i = 1, 2, ..., 2048) with respect to the excitation flash (Figure 2). Their width c is adjustable between 50 ns and 1 s, depending on the required time resolution in the experiment.

The counting proceeds as follows. In a given channel window C_i, photopulses are counted only if C_i overlaps with the modulation time window L and/or R. If there is overlap with L, the number of counts is stored with a plus sign in C+ and C−; if overlap is with R, the number of counts is stored with a plus sign in C+ and with a minus sign in C−. The contents of the counters is transferred to two multichannel memories which then contain the values of C− and C+ for all channels i. These data sets contain the information on the differential luminescence intensity ($I_L - I_R$) and the total intensity ($I_L + I_R$), respectively, and thus on g_{lum} as a function of time. It is possible to switch off the modulation window shaper if one is interested only in the decay of the total luminescence intensity. In the cw mode of the spectrometer, the flash lamp is replaced by a Xenon arc lamp, and both multichannel counters act as single counters which count during a preset period of time (mostly on the order of seconds).

Experimental Determination of the Two Bimolecular Rate Constants Describing the Enantioselective Quenching

$Ln(dpa)_3^{3-}$ complexes, abbreviated Ln here, have (approximate) D_3 symmetry,[33] and there is spectroscopic evidence that this symmetry is retained in solution.[34] Having the shape of a three bladed propeller, they occur in two enantiomeric forms, Δ-Ln and Λ-Ln (see Figure 1). In aqueous solution at room temperature, the rate of enantiomeric interconversion is ∼10 s^{-1} (measured for $Eu(dpa)_3^{3-}$ in the excited state),[35] and hence, Ln occurs as an equimolar mixture of the Δ-Ln and Λ-Ln enantiomers (racemic mixture). The interconversion process is slow compared to the decay of the excited state of Eu* and Tb* (decay rate on the order of 10^3 s^{-1}), and so, in the present

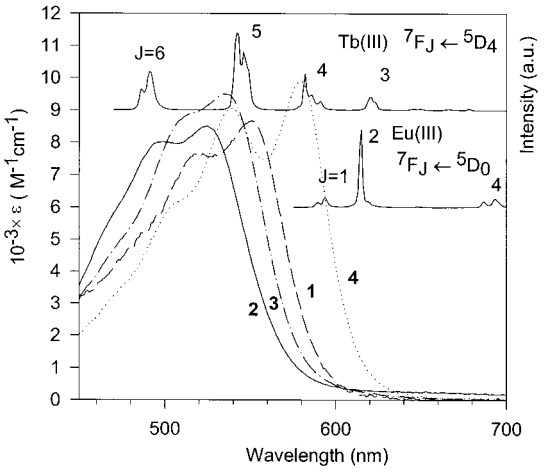

Figure 3. Photoluminescence spectrum of Tb and $Eu(dpa)_3^{3-}$ with spectroscopic assignments. Absorption spectra of the corrinoids **1**−**4**.

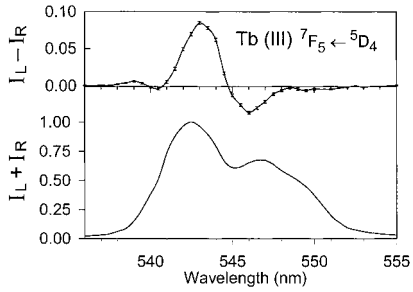

Figure 4. Total intensity (bottom) and circular differential intensity (top) of $Tb(dpa)_3^{3-}$ $^7F_5 \leftarrow {}^5D_4$ emission in the presence of ferricytochrome *c* protein. Experimental conditions: [Tb] = 1.0 mM, [cytc] = 11 μM, I = 0.012 M, unbuffered solution, pH∼7, spectral resolution 1 nm. The vertical bars represent the standard errors in the accumulated $I_L - I_R$ data points.

quenching studies, racemization occurring in the excited state may be neglected.

The lanthanide species under study luminesce efficiently exhibiting a series of rather narrow electronic bands characteristic of the lanthanide 4f−4f transitions (see Figure 3). Being racemic, a solution of Ln exhibits no CPL (if the excited state is populated with unpolarized excitation light). Addition of small quantities (∼micromoles) of an enantiomerically resolved quencher species to the racemic solution of Ln (∼millimoles) can induce a strong CPL. Lanthanide transitions with $\Delta J = \pm 1,0$, obeying the magnetic dipole selection rule, show the strongest circular polarization. As an example, the Tb(III) $^7F_5 \leftarrow {}^5D_4$ transition is shown in Figure 4. Under these conditions, no circular dichroism for the lanthanide transitions is observed, indicating that in the ground state, the racemic equilibrium has not been disturbed. Significantly, the band shape of the circular differential intensity is the same as that observed for a racemic Ln solution upon circularly polarized excitation, which creates an enantiomeric excess in the excited state ([Δ-Ln*] ≠ [Λ-Ln*]) due to the CD effect. This indicates that the net circular polarization induced by Q results from a difference in luminescence efficiency of the two Ln enantiomers.

Time-resolved CPL measurement have given compelling evidence for these inferences. A pulse of unpolarized excitation light produces an excited state population of Ln* which is initially racemic. A chiral quencher Q may quench [Δ-Ln*] faster than [Λ-Ln*], and this results in an enantiomeric excess in the excited state which grows with time after the excitation pulse (whereas, of course, the total concentration, [Δ-Ln*] + [Λ-Ln*], decays with time).

More quantitatively the energy transfer reaction may be written schematically

$$\sigma\text{-Ln}^* + \text{Q} \xrightarrow{k_q^\sigma} \sigma\text{-Ln} + \text{Q}^* \tag{3}$$

$$k^\sigma = k_0 + k_q^\sigma[\text{Q}] \tag{4}$$

In eq 3, σ labels the chirality (Δ or Λ) of Ln, and Q denotes the chiral quencher.

The excited-state population of a single Ln enantiomer, σ-Ln*, is expected to decay strictly exponentially (∼exp($-k^\sigma t$)) with a decay constant as given by (4). In the absence of Q the decay constants k^σ reduce to k_o, the reciprocal lifetime of Ln*, which is by symmetry the same for the two enantiomers. In the case of enantioselectivity, the quenching rate constants k_q^σ are different for the two optical isomers, leading to different lifetimes of Λ-Ln* and Δ-Ln* in the presence of Q i.e. to a biexponential decay of the luminescence intensity (see eq 5). Anticipating a fitting procedure to experimental data, we have included in eq 5 a term which can take into account the dark counts of the photon counting detector.

The two differing quenching rate constants k_q^Δ and k_q^Λ also give rise to a CPL effect which changes with time after pulsed unpolarized excitation at $t = 0$ according to eq 6

$$I(t) = A\{\exp(-k^\Delta t) + \exp(-k^\Lambda t)\} + \text{dark counts} \tag{5}$$

$$g_{lum}(\lambda,t) = g_{lum}^\Lambda(\lambda)\tanh(^1/_2 k_d[\text{Q}]t) \tag{6}$$

In this equation $k_d = k_q^\Delta - k_q^\Lambda$, tanh denotes the hyperbolic tangent function and $g_{lum}^\Lambda(\lambda)$ the (wavelength dependent) degree of circular polarization of the pure Λ-Ln enantiomer.

The degree of enantioselectivity in the quenching, E_q, is usually expressed as eq 7. It varies between $-1 \le E_q \le +1$, where the boundary values apply when the reaction is completely enantioselective

$$E_q = (k_q^\Delta - k_q^\Lambda)/(k_q^\Delta + k_q^\Lambda) = k_d/2k_q^{avg} \tag{7}$$

The equation at the right side of eq 7 also defines the average quenching rate constant $k_q^{avg} = {}^1/_2(k_q^\Delta + k_q^\Lambda)$.

The correctness of these theoretical expressions describing the enantioselective quenching has been evaluated experimentally for a variety of quenchers, and below, we discuss experiments involving $Tb(dpa)_3^{3-}$ and vitamin B_{12} (abbreviated to **1**, cf Scheme 1). To illustrate the spectroscopic transitions involved, we show the luminescence spectra of $Tb(dpa)_3^{3-}$ and $Eu(dpa)_3^{3-}$ along with the absorption spectra of some quenchers of vitamin B_{12} type in Figure 3. In Figure 5, typical time-resolved luminescence data obtained for an aqueous (0.42 M) solution of $Tb(dpa)_3^{3-}$ with a small quantity (19 μM) of **1** at room temperature are given. The thin line E represents the luminescence decay of the system in the absence of quencher. It yields the value of k_0 (cf eq 4). Addition of B_{12} results in a drastic shortening of the lifetime of Tb*; see the data points (D). A fit of eq 5 to these data, taking into account the value of k_o, yields the values 1.3×10^8 $M^{-1}s^{-1}$ and 0.77×10^8 $M^{-1}s^{-1}$ for the pair (k_q^Δ,k_q^Λ). Thus, we obtain the result $k_d = -5.0 \pm 0.5 \times 10^7$ $M^{-1}s^{-1}$.

Figure 6 shows a Stern−Volmer plot of the Tb* luminescence quenched by **1**. At each quencher concentration, a pair of decay constants (k_q^Δ,k_q^Λ) is found from a fit of eq 5 to the experimental data. Both depend linearly on [**1**], and from the slopes, one finds the values $k_q^\Lambda = 1.3 \times 10^8$ $M^{-1}s^{-1}$, $k_q^\Delta = 0.77 \times 10^8$

SCHEME 1

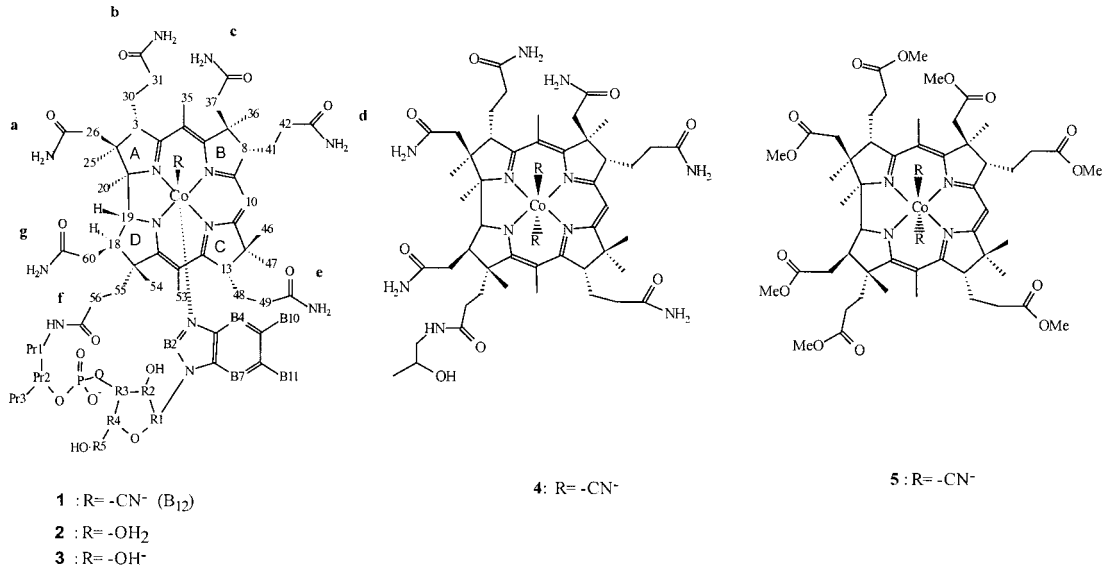

1 : R= -CN⁻ (B_{12})
2 : R= -OH_2
3 : R= -OH⁻

4: R= -CN⁻

5 : R= -CN⁻

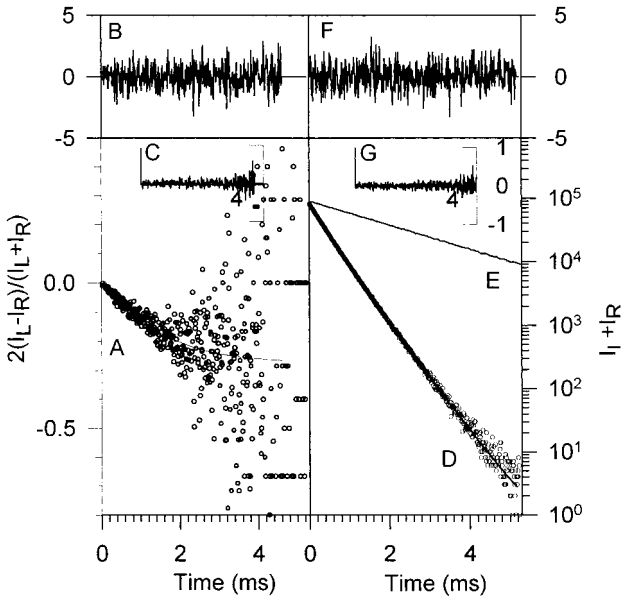

Figure 5. Time-resolved circular polarization g_{lum} (left; A) and decay of total intensity (right, D) of $Tb(dpa)_3^{3-}$ luminescence in the presence of **1** monitored at 542.8 nm (spectral bandwidth 2 nm). The solid line at A represents a nonlinear least-squares fit of eq 6 to the CPL data; the intensity decay data (D) are fitted to eq 5. B and F are the weighed residuals and C and G their autocorrelation functions. The thin line E shows the decay of the luminescence in the absence of quencher. Sample conditions: $[Tb(dpa)_3^{3-}] = 0.42$ mM, [**1**] =19 μM.

$M^{-1}s^{-1}$, and, subsequently, $k_d = -5.0 \times 10^7$ $M^{-1}s^{-1}$. The regular behavior of k_q^σ in the Stern−Volmer plots supports the adequacy of the biexponential analysis. Previously, it has been shown that fitting of eq 5 to experimental decay curves yields accurate values for the two decay constants, provided that they differ by more than 5% and that enough signal has been accumulated.[13]

The time-resolved CPL data of the $Tb(dpa)_3^{3-}$/**1** system in Figure 5 show that right after the excitation pulse, the lanthanide luminescence is not circularly polarized, implying that the Tb* population can, at this point in time, still be regarded as racemic. With time after excitation, g_{lum} changes to negative values, indicating that the Tb* population becomes gradually "enriched" in the Δ enantiomer. (For Tb- and $Eu(dpa)_3^{3-}$, a correlation

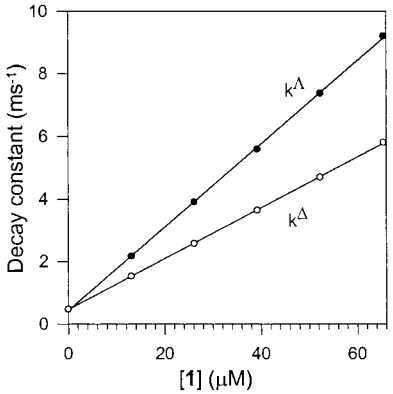

Figure 6. Stern−Volmer plot of the quenching of $Tb(dpa)_3^{3-}$ luminescence (0.21 mM) by **1**. At each concentration, a pair of diastereomeric decay constants is found by fitting eq 5 to the experimental decay curve. The solid lines represent linear regressions to the data.

between the sign of $g_{lum}(\lambda)$ and the absolute configuration has been made).[13] From a fit of eq 6 to the CPL data of Figure 5, we obtain $k_d = -5.2 \pm 0.5 \times 10^7$ $M^{-1}s^{-1}$, in good agreement with the value obtained from analysis of the luminescence decay data.

From a fit of eq 7 to the observed circular polarization, one also finds the dissymmetry factor of the Λ-enantiomer of $Tb(dpa)_3^{3-}$: $g_{lum}^\Lambda = +0.27 \pm 0.02$ (at 542.8 nm emission wavelength, bandwidth 4 nm). If the experimental uncertainty is taken into account, the latter value is equal to the values determined earlier using ferri cytochrome *c* ($g_{lum}^\Lambda = +0.30 \pm 0.01$)[23] and $Ru(phen)_3^{2+}$ ($g_{lum}^\Lambda = +0.28 \pm 0.02$)[13] as the quencher. This again illustrates the consistency of our description of the quenching process.

Finally, the analysis of the experimental data provides the following value of the enantioselectivity in the quenching of $Tb(dpa)_3^{3-}$ luminescence by **1**: $E_q = -0.24$ where we have used eq 7.

Mechanistic Model of the Quenching Reaction

In most studies of the enantioselective excited-state quenching of $Ln(dpa)_3^{3-}$, the following kinetic scheme was adopted to describe the quenching reaction: Free Δ-Ln and Λ-Ln species

SCHEME 2

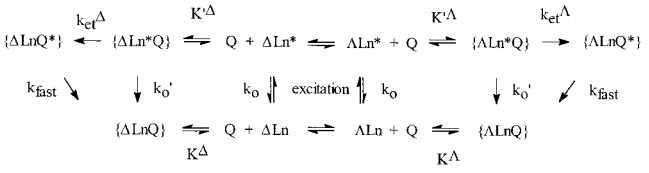

are promoted to the luminescent state by the absorption of (pulsed) unpolarized excitation light. Apart from free Ln ions, complexes with the quencher, $\{\sigma\text{-LnQ}\}$, may also be present in the sample. Given the typical concentrations used (μM for the quencher, mM for Ln), the concentration of σ-LnQ complexes is negligible compared to Ln, and direct excitation of $\{\sigma\text{-LnQ}\}$ may be ignored. Under certain circumstances, $[\{\sigma\text{-LnQ}\}]$ may be considerable when compared to [Q], and this may affect the quenching rate.[15,23]

The decay of Tb* and Eu* occurs on a microsecond time scale (k_o) which allows for diffusion of Ln* over considerable distances through the solution. The σ-Ln* species may associate with Q to form an encounter complex $\{\sigma\text{-Ln*Q}\}$ with rate constant k^{σ}_{diff}. This encounter pair may dissociate again (rate $k^{\sigma}_{-\text{diff}}$). The equilibrium constant for encounter pair formation is defined as $K'^{\sigma} = k^{\sigma}_{\text{diff}}/k^{\sigma}_{-\text{diff}}$. The encounter pair may also undergo (internal) energy transfer with a rate k^{σ}_{et}. As most quenchers are nonfluorescent, the energy transfer step is likely to be followed by rapid decay of Q* (k_{fast} in Scheme 2), preventing the occurrence of back energy transfer from Q* to Ln.

Applying the steady-state conditions to $[\{\sigma\text{-Ln*Q}\}]$ and assuming that the rates k_{diff} and $k_{-\text{diff}}$ are large compared to k_{et}, which in turn is much larger than k_o' (which is expected to be equal to k_o), we find eq 8

$$k^{\sigma}_{q} = K'^{\sigma} k^{\sigma}_{\text{et}} \tag{8}$$

This formula reflects that the chiral discrimination in the quenching can result from enantioselectivity in the binding (K'^{σ}), from enantioselectivity in the energy transfer (k^{σ}_{et}) or from a combination of these two.

If k_{et} and $k_{-\text{diff}}$ have comparable magnitudes, the quenching rate approaches the diffusional limit, and eq 8 is no longer appropriate; it should replaced by eq 9

$$(k^{\sigma}_{q})^{-1} = (K'^{\sigma} k^{\sigma}_{\text{et}})^{-1} + (k^{\sigma}_{\text{diff}})^{-1} \tag{9}$$

In the extreme case of complete diffusion control ($k^{\sigma}_{q} = k^{\sigma}_{\text{diff}}$), the enantioselectivity is expected to be vanishingly small since the diffusion rate may be assumed to be equal for the two enantiomers ($k^{\Delta}_{\text{diff}} = k^{\Lambda}_{\text{diff}}$) when an achiral solvent is used. Reduction of the enantioselectivity in the quenching of $Tb(dpa)_3^{3-}$ by $Ru(phen)_3^{2+}$ in methanol solution at very low ionic strength has been interpreted in terms of partial diffusion control.[14]

The excitation to the lowest excited states of Tb, Eu, and $Dy(dpa)_3^{3-}$ involves mainly the inner 4f electrons, which are not involved in the binding of the ligands to the central Ln(III) atom. Therefore, these chelates are not expected to appreciably change their geometry upon excitation, and the binding properties of a $Ln(dpa)_3^{3-}$ species may be assumed to be the same in its ground and excited state, i.e., $K^{\sigma} = K'^{\sigma}$. Thus, for the study of the energy transfer reaction, the ground-state lanthanide chelate provides an ideal, unreactive model compound which may be used to study separately the enantioselectivity in the binding of the reactants. This feature we will use later on.

TABLE 1: Enantioselectivity and Average Rate Constant for Quenching of Luminescence from $Eu(dpa)_3^{3-}$ and $Tb(dpa)_3^{3-}$ by Metalloproteins in Water[a] [23,24,26]

		Tb		Eu	
protein		E_q	$10^{-7} \times k_q^{\text{avg}}$ ($M^{-1}s^{-1}$)	E_q	$10^{-7} \times k_q^{\text{avg}}$ ($M^{-1}s^{-1}$)
cytochrome *c*	horse	+0.27	15	+0.48	7.5
	cow	+0.28		+0.48	
	chicken	+0.24		+0.45	
	pigeon	+0.23		+0.44	
	tuna	+0.14	(17)[e]	+0.20	(7.5)[e]
cytochrome *c*-550[b]	wild type	+0.17	21	+0.20	7.6
	Lys14 → Glu	+0.19	7.4	+0.22	2.3
	Lys99 → Glu	+0.07	5.7	+0.10	1.7
azurin[c]	wild type	n.d.	~0.05	+0.11	0.3
	Met44 → Lys	+0.11	0.7	+0.12	1.7
amicyanin[b]	wild type	n.d.	n.d.	+0.05	11
plastocyanin[d]	wild type	n.d.	n.d.	n.d.	~0.05

[a] Conditions: ionic strength I = 22 mM, pH 7.2, lanthanide concentration 1 mM, T = 293K. [b] From *Paracoccus versutus* (formerly, *Thiobacillus*). [c] From *Pseudomonas aeruginosa*. [d] From Parsley leaves. [e] Calculated assuming the same extinction coefficient as for the protein from horse.

The chelates involving the trivalent lanthanide ions Nd, Eu, Gd, and Tb can, to a good approximation, be regarded as isostructural,[36] and their charge distributions can be assumed to be the same. This then implies that the binding properties of chelates with different central Ln ions can be regarded as virtually the same (i.e., $K^{\sigma}_{\text{Tb}} = K^{\sigma}_{\text{Eu}} = K^{\sigma}_{\text{Nd}}$). In studies involving $Ln(dpa)_3^{3-}$ complexes, this feature allows us to choose that central Ln atom which is most suited for a particular spectroscopic technique (vide infra).

Study of the Relation between Structure and Enantioselectivity: Quenching by Metalloproteins

As mentioned, a main question is how the reactivity in the energy transfer is related to the molecular structure of the reactants. To this end, we have studied the selective quenching displayed by a series of structurally related metalloproteins belonging to the class of *c*-type cytochromes. Mitochondrial cytochrome *c* is a small metalloprotein containing a heme group with the Fe ion in either the di- or trivalent state. The protein is an efficient quencher of $Ln(dpa)_3^{3-}$ luminescence[37] and was later found to discriminate between Δ-Ln and Λ-Ln in this energy transfer reaction.[23] The efficiency of quenching can be related to the presence of anion binding sites on the protein located near the so-called exposed heme edge. This is a site on the surface of the protein where an edge of the heme group is exposed to the solvent. It has been implicated in electron-transfer reactions, and therefore, this part of the protein surface has been regarded as the active site.[38] In Table 1, we have listed values for E_q and k_q^{avg} for the ferric form of the protein obtained from various sources. For the proteins from mammals, we find high enantioselectivities, especially with $Eu(dpa)_3^{3-}$ as luminophore. For Tb, a significantly lower value is found. Studies of the temperature and pressure dependence of the quenching reaction revealed that the transition states involved in the energy transfer process are indeed different for the Tb and Eu chelates.[24] In addition, differences in the pH dependence of the quenching were also observed.[25]

The amino acid sequence of the proteins from horse and cow appears to differ in only three amino acids residues.[38] Appar-

ently, these differences do not affect the enantioselectivity, and therefore, the differing amino acid residues are not involved in interactions with the luminophore. The selectivity displayed by two avian proteins (pigeon, chicken) is almost the same as that for horse protein, even though the proteins from birds differ in 11 amino acid residues from horse cytc. For tuna, we find a significant change in selectivity, and interestingly, the primary structure of this protein differs most from that of horse protein (19 different residues). From the X-ray structures of the horse[39] and tuna[40] proteins, it is known that the fold of the proteins is very similar. Apparently, the chiral discrimination is to a large extent controlled by particular amino acid residues at the protein surface. The extinction coefficients for the proteins other than that from horse protein are not available, but assuming that the extinction coefficient for tuna is the same as that for horse protein, one calculates quenching rate constants which are virtually identical for both proteins, indicating that the rates do not vary strongly with protein structure.

Also listed in Table 1 are the data for structurally related bacterial cytochrome *c*-550 from *Paracoccus versutus*.[41] The E_q for the wild-type protein has the same sign as that for the eucariotic proteins. For this bacterial protein, site-specific mutants have been genetically engineered.[42] Mutation of the positively charged lysine 99 to a negatively charged glutamate significantly lowers the quenching rate. This can be interpreted in terms of electrostatic forces influencing the binding energy of Ln to the surface area of the protein around the exposed heme edge. Lysine 99 is a surface residue close to the heme group. Surprisingly, mutation of Lysine 99 also results in a change of the enantioselectivity, indicating that this residue interacts directly with the Ln chelate in the transition state of the quenching reaction. Mutation of Lys 14, also close to the heme edge, results in a reduction of the quenching rates but hardly influences the enantioselectivity. This indicates that Lys 14 is not in direct contact with the $*Ln(dpa)_3^{3-}$ species in the transition state but, rather, interacts through long-range electrostatic forces.

Table 1 also contains quenching parameters for some blue copper proteins.[26] The enantioselectivities are not as high as for those the cytochromes *c*, and the quenching rate constants vary strongly with the protein structure despite a very similar structure of the chromophoric unit in the protein, i.e., the copper center. For azurin, mutation of methionine 44 to a positively charge lysine enhances the quenching but hardly influences the selectivity. Interestingly, all proteins listed in the table prefer the Δ-Ln enantiomer in their quenching. In the course of our research we also found one protein which shows opposite enantioselectivity: myoglobin from horse ($E_q = +0.24$).[43]

The main conclusion from the data in Table 1 is that the activity and selectivity of the quencher is to a large extent controlled by interactions between the luminophore and surface residues of the protein close to the metal center. As the lanthanide chelate is a highly charged species, it is no surprise that the replacement of a lysine residue, which normally carries a positive charge at physiological pH, by a glutamate, which has a negative charge, strongly reduces the quenching rate. Also, the dependence of the quenching rates on ionic strength changes upon mutation, and this has been interpreted in terms of an electrostatic model.[23] Changes of the enantioselectivity upon modification of a single residues as observed for the bacterial cytochrome *c* provides strong evidence for specific interactions between the luminophore and a few surface residues controlling the selectivity. Such changes in chiral discrimination have also been observed for oxidation reactions catalyzed by cytochrome P450 2D-6. Here, it was found that modification of singles residues close to the active site of this enzyme can either alter the enantioselectivity[44] or leave it uninfluenced.[45] Variation in selectivity with the origin of the enzyme (from humans or monkeys)[46] has also been observed. Such variation is then usually interpreted in terms of a lock-and-key model, in which the substrate binds to a particular well-defined site on the protein surface. If replacement of a particular amino acid residue influences the selectivity, it is implicated in the binding site. The observation of changes in the enantioselectivity in the energy transfer reaction upon modification of a single residue might well indicate that also here a lock-and-key model applies. The enantioselective quenching may then be used to investigate local structural changes induced by, e.g., temperature or pH at the active site of the metalloprotein acting as quencher. For cytc, known conformational transitions are indeed reflected by changes in quenching rate and selectivity.[24,25]

When the two step model (see above) is adopted for the energy transfer reaction, the question arises whether the enantioselectivity results from selectivity in the binding of the substrate to the protein or from the actual activated reaction step following this binding.

TABLE 2: Enantioselectivity and Average Rate Constant for Quenching of $Eu(dpa)_3^{3-}$ and $Tb(dpa)_3^{3-}$ Luminescence by Vitamin B_{12} Derivatives in Water[28]

	$Tb(dpa)_3^{3-}$		$Eu(dpa)_3^{3-}$	
	E_q	$10^{-7} \times k_q^{avg}$ ($M^{-1}s^{-1}$)	E_q	$10^{-7} \times k_q^{avg}$ ($M^{-1}s^{-1}$)
1	−0.24	10	−0.27	0.41
2[a]	−0.23	53	−0.21	38
3[b]	−0.27	13	−0.29	3.6
4	−0.20	29	−0.29	7.3
5	+0.01	5.1	+0.02	1.2

[a] pH 6.7, Hepes buffer 9.5 mM, ionic strength $I = 8$ mM. [b] pH 8.9, Ches buffer 9.5 mM, $I = 8$ mM. Other systems neutral pH, $I = 5$ mM.

Enantioselective Quenching by Vitamin B_{12} Derivatives

In an attempt to learn more about the origin of the enantiodifferential quenching, we have turned to a simpler donor−quencher system: $Ln(dpa)_3^{3-}$ and vitamin B_{12}.[28,29,47] Attractive features of this quencher are that various derivatives of B_{12} are commercially available, and the spectroscopic properties of these corrinoids have been well studied.[48] The structural formulas are given in Scheme 1, and the quenching data are listed in Table 2.

As can be seen, the enantioselectivity changes only very little when in **1** the axial ligand R of the cobalt atom is changed from cyanide to a water molecule (**2**). The coordinated water molecule can lose a proton, and a pK_a value of 7.6 has been determined for this transition.[49] At low pH, the quencher has a net 1+ charge, while at higher pH, the complex has zero net charge. In reactions with the triply negative charged donor, this difference in charge is reflected in the higher quenching rate for the low pH form. It also gives rise to a different dependence of the quenching rate on ionic strength for the acid and conjugated base form of the quencher.[28] Surprisingly, when in B_{12} the bulky dimethyl benzimidazole ligand is exchanged for a cyanide (**4**), the enantioselectivity is only slightly affected. When, however, the amide groups on the side chains are replaced by ester moieties, E_q drops to zero. This leads to the hypothesis that hydrogen bonding interactions between the amide protons on the side chains of the corrin ring and the carboxylate groups of the dpa ligands are a determining factor for the enantioselectivity.

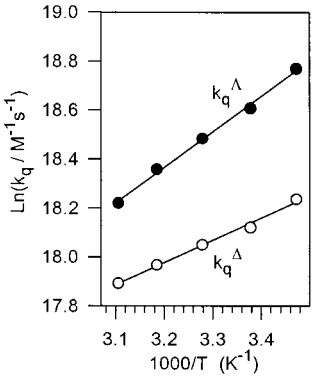

Figure 7. Temperature dependence of the quenching rate constants of the system **1**/Tb(dpa)$_3^{3-}$. Quenching rate constants are determined by analysis of the decay of the total emission monitored at 542.8 nm (2 nm). Sample conditions: [Tb(dpa)$_3^{3-}$] = 0.21 mM; [**1**] = 64 μM.

Further information on the donor−quencher interactions comes from analysis of the temperature dependence of the quenching rates. As illustrated in Figure 7, the rates show a decrease with increasing temperature, and hence, a negative activation energy is associated with the reaction. Such negative activation energies have also been observed for the Tb(dpa)$_3^{3-}$/Ru(phen)$_3^{2+}$ system[15] and are consistent with the occurrence of a precursor complex in the quenching reaction sequence. When formation of such an encounter complex is exothermic, an increase of temperature implies that the lifetime and relative concentration of these precursor complexes are reduced. When the activation energy of the energy transfer is smaller than the formation enthalpy of the precursor complex, a negative activation energy is observed for the overall reaction. Assuming that the actual energy transfer reaction step has negligible activation energy, the stability of the complexes may be estimated from the observed activation energies: −12 kJ/mol for the Λ-enantiomer and −7 kJ/mol for the Δ-form. For the quenching by the ester derivative **5**, both activation energies are +0.3 (±0.2) kJ/mol, consistent with the idea that in this case the precursor pair lacks stabilization by hydrogen bond formation.

Enantioselectivity in the Binding of Ground-State Ln(dpa)$_3^{3-}$ to B$_{12}$

In this section, we describe how NMR and CD techniques can be of help to get information on the enantioselectivity in the binding of ground-state Ln(dpa)$_3^{3-}$ to B$_{12}$.

NMR.[47] In the series of trivalent lanthanide ions, the magnetic properties show a rich variation. For instance, the magnetic moment of La(III) is zero, but for others (Tb(III) and Gd(III)), it is quite high.[50] In Tb(dpa)$_3^{3-}$, the magnetic susceptibility is anisotropic, and the electron spin relaxation time is short; hence, it can be used as an NMR shift reagent. In Gd(dpa)$_3^{3-}$, the 4f shell is half filled, and the magnetic susceptibility is isotropic, while in addition the electron spin relaxation time is long. Due to these factors, a Gd chelate does not shift the NMR frequency of nearby protons but can efficiently enhance their relaxation rates.[51]

Addition of Tb(dpa)$_3^{3-}$ to solutions of B$_{12}$ in D$_2$O leads to a shift of the nuclear magnetic resonance frequency of certain protons of the corrinoid, whereas the diamagnetic La(dpa)$_3^{3-}$ has no effect.[47] These lanthanide-induced shifts (LIS) appear to be largest for protons located near the side chains a and g, viz. protons attached to the carbon atoms 18,19, 25, 26, 54, and 60 (cf. Scheme 1). The shifts are larger for **2** than for **1**, but their relative magnitudes are distributed similarly in the spectrum. This shows that Tb(dpa)$_3^{3-}$ binds to the corronoids with a rather specific geometry.

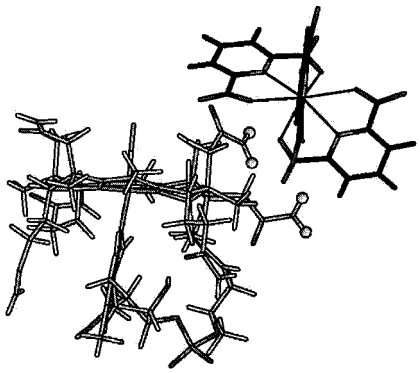

Figure 8. Molecular modeling of the {Λ-Tb(dpa)$_3^{3-}$:B$_{12}$} complex obtained by energy minimization of the a and g side chains, with Tb(dpa)$_3^{3-}$ in the relative position found from the fit of the LIS data of **2**, while keeping the rest of the corrinoid frozen. Amide protons of the a and g side chains of B$_{12}$ are indicated by gray spheres.

More detailed information on the complexation was obtained from a quantitative analysis of the observed shifts. The $\sim D_3$ symmetry of Ln(dpa)$_3^{3-}$ species implies a unique magnetic axis, parallel to the 3-fold symmetry axis.[36] For such chelates, the dipolar or pseudocontact contribution to the induced shift for a B$_{12}$ proton i ($\Delta\delta_i$) with fixed position relative to the Ln(dpa)$_3^{3-}$ can be written as[36,52]

$$\Delta\delta_i = D'_{\mathrm{Ln}} \frac{3\cos^2\theta_i - 1}{R^3_{\mathrm{Ln}-i}} \frac{[\{\mathrm{LnQ}\}]}{[\mathrm{Q}_0]} \qquad (10)$$

The magnitude of the shift depends on the distance between i and the Ln ion ($R_{\mathrm{Ln}-i}$) and on the angle θ_i between the magnetic axis of the Ln complex and the vector $\mathbf{R}_{\mathrm{Ln}-i}$. In eq 10, D'_{Ln} is a constant which depends on the anisotropy of the paramagnetic susceptibility tensor of the Ln chelate.

A fit of eq 10 to the observed shifts yields the distance and the orientation of the magnetic axis of the lanthanide chelate relative to the protons on B$_{12}$. With these results, we found, using molecular modeling techniques, that Tb(dpa)$_3^{3-}$ is within hydrogen bonding distance of the a and g side chains of **1** (and **2**). Formation of multiple hydrogen bonds between the protons on the amide and the carboxylate groups of the dpa ligands is possible. This is illustrated in Figure 8 for the ΛLn−B$_{12}$ complex. It should be remembered that because of the rapid exchange on the NMR time scale of Ln in the Ln−B$_{12}$ complex, the measured induced shifts are actually an average of the shifts of the ΔLn−B$_{12}$ and the ΛLn−B$_{12}$ encounter complex.

If the value of D'_{Ln} in eq 10 is known, it is also possible to extract information on the magnitude of the association constant from the LIS data. In the case of rapid chemical exchange of free and bound Q, the induced shift is proportional to [{LnQ}]/[Q$_0$], i.e., the mole fraction of bound Q (x), which relates via eq 11 to the association constant K

$$K = \frac{[\{\mathrm{LnQ}\}]}{[\mathrm{Ln}][\mathrm{Q}]} = \frac{x}{1-x}\frac{1}{([\mathrm{Ln}]_0 - x[\mathrm{Q}]_0)} \qquad (11)$$

So if x can be determined from the observed shifts, the value of K can be calculated, given the initial concentrations [Ln]$_0$ and [Q]$_0$. An estimate of the value of D'_{Ln} can be made from the LIS data of the protons on the dpa ligand. Magnetic properties of the Ln(dpa)$_3^{3-}$ chelates have been studied extensively, and it has been concluded that the induced shifts of the

TABLE 3: Average Binding Constants K^{avg} of Tb(dpa)$_3^{3-}$ and B_{12} Derivatives from NMR Spectroscopy[b]

	K^{avg} (M^{-1})	$K^{\Delta} - K^{\Lambda}$ (M^{-1})	E_b
1	3 ± 0.6	-4.4 ± 0.5	-0.7 ± 0.2
2[b]	22 ± 5	-28 ± 3	-0.6 ± 0.2
4	0.6 ± 0.2	-0.9 ± 0.3	-0.7 ± 0.3

[a] Difference in binding constants of Λ and Δ-Nd(dpa)$_3^{3-}$ and B_{12} derivatives from CD spectroscopy. Enantioselectivity in the binding E_b.[47] [b] pH 6.7, $I = 0.12$M.

dpa protons result from dipolar interactions with only a minor contribution from the contact mechanism.[53] The positions of the dpa protons relative to the Ln(III) ion are known from X-ray studies so that the magnitude of the parameter D'_{Ln} can be determined.

The binding constants obtained in this way are listed in Table 3. Again, because of the rapid exchange, they are in fact an average of the values for the Δ and Λ enantiomers of Ln(dpa)$_3^{3-}$, i.e., $K^{avg} = (K^{\Delta} + K^{\Lambda})/2$. The stronger binding of **2** to the negatively charged lanthanide species can be rationalized in terms of a favorable electrostatic interaction with the positively charged corrinoid. A net 1+ charge for **2** at low pH is supported by measurements of the ionic strength dependence of the luminescence quenching rates.[28] The magnitudes of the proton relaxations induced in **1** by Gd(dpa)$_3^{3-}$ are consistent with the geometry and the magnitude of K^{avg} found from the LIS analysis.

While the NMR measurements provide valuable information on the complexation (the technique is currently also receiving attention from other research groups),[54] they yield no information on the enantioselectivity in the binding. To study this aspect we have turned to circular dichroism measurements.

Induced CD. [47] Addition of an enantiomerically pure species Q to a solution of a (labile) racemate may result in a shift of the 1:1 enantiomeric equilibrium of the latter (Pfeiffer effect). The phenomenon may be abstracted by the following scheme (cf lower line of Scheme 2):

$$\{\Delta\text{LnQ}\} \underset{K^{\Delta}}{\rightleftharpoons} \text{Q} + \Delta\text{Ln} \underset{K_{rac}=1}{\rightleftharpoons} \Lambda\text{Ln} + \text{Q} \underset{K^{\Lambda}}{\rightleftharpoons} \{\Lambda\text{LnQ}\}$$

Following Huskowska and Riehl,[55] who have given a quantitative description of the effect, one may assume that the lanthanide chelates (Ln) can associate with Q to form Δ-LnQ and Λ-LnQ complexes. The complexation is taken to be "outer sphere", meaning that the first coordination sphere Ln remains the same upon binding to Q so that the optical properties of the Ln are hardly affected. It may also be assumed that the energy of the uncomplexed Ln species is not influenced by the chiral agent. Therefore, the concentrations of free Δ-Ln and Λ-Ln are taken equal i.e., $K_{rac} = 1$. Due to enantiodifferentiating interactions between Ln and Q, the free energies of the two (LnQ) diastereomers may differ, i.e., $K^{\Delta} \neq K^{\Lambda}$, leading to a difference in concentration and hence a nonvanishing circular dichroism in the lanthanide transitions. Thus, observation of induced circular dichroism (ICD) in the absorption bands of Ln(dpa)$_3^{3-}$ complexes upon addition of B_{12} might give important experimental evidence on the enantioselectivity in the binding of the lanthanide chelate to the quencher.

Experimentally, the detection of the induced CD is difficult for the Tb and Eu chelates, as their weak absorptive transitions are buried in the strong and broad absorption bands of the B_{12} quenchers. Moreover, the strong quenching of the luminescence prohibits measurement of the shift of the ground-state racemic equilibrium by CPL techniques. To study the ICD, we therefore have made use of Nd(III)(dpa)$_3^{3-}$, which has appropriate optical transitions in a wavelength region where B_{12} absorbs light only very weakly ($^4I_{9/2} \rightarrow {}^4F_{9/2}$ ($\sim$660 nm), $^4I_{9/2} \rightarrow {}^4F_{7/2}$ ($\sim$735 nm), and also $^4I_{9/2} \rightarrow {}^2H_{9/2}$ ($\sim$795 nm)). These transitions obey the magnetic dipole selection rule ($\Delta J = \pm 1,0$), and one may therefore expect large degrees of circular polarization in absorption.[30h] Combined with the fact that the oscillator strengths of these Nd transitions are relatively large as compared to the other lanthanides, this makes Nd chelates very promising for our ICD studies.

Upon the addition of **1**, **2**, or **4**, in quantities large in comparison to those used in the quenching experiments (millimoles vs micromoles), ICD is indeed observed for the Nd(III) transitions in the spectral range 700−810 nm. The band shapes of the CD induced by the B_{12} derivatives appear to be the same as that induced by various other known Pfeiffer agents, and thus, the circular dichroism can be attributed to an excess of one enantiomer of Nd(dpa)$_3^{3-}$ induced by outer sphere coordination to the corrinoids **1**, **2**, or **4**. The sign of the ICD shows that the B_{12} derivatives bind preferentially to Λ-Ln.

In the limit of low quencher concentration the magnitude of the induced circular dichroism can be expressed as[47]

$$\Delta A = (\Delta\epsilon^{\Delta} cl) \frac{(K^{\Delta} - K^{\Lambda})}{2} [\text{Q}] \qquad (12)$$

Here c denotes total concentration of Ln, l the optical path length, $\Delta\epsilon^{\Delta}$ denotes the circular dichroism for the pure Δ enantiomer of Nd(dpa)$_3^{3-}$, which can be estimated.[47] Measuring the magnitude of the induced CD as a function of the quencher concentration then yields values for the differential binding constant $K^{\Delta} - K^{\Lambda}$ (see Table 3). By combining the results of the ICD and NMR measurements, it is possible to calculate a value for the enantioselectivity in the binding, E_b, which is defined by

$$E_b = \frac{K^{\Delta} - K^{\Lambda}}{K^{\Delta} + K^{\Lambda}} = \frac{K^{\Delta} - K^{\Lambda}}{2K^{avg}} \qquad (13)$$

For **1**, **2**, and **4** the E_b values are also listed in Table 3. Comparing the data in the Tables 2 and 3, it follows that for all three compounds the signs of E_b and E_q are the same. So the B_{12} derivatives prefer the Λ enantiomer of the lanthanide chelate in both binding and quenching. Surprisingly, values for $|E_b|$ are found to be higher than corresponding values for $|E_q|$.

Energy Transfer Mechanism

To interpret the disparity between E_b and E_q, we assume that the binding constants for the excited and ground-state lanthanide chelate are the same (see above) and write eq 13

$$k_q^{\Lambda}/k_q^{\Delta} = (\text{K}^{\Lambda}/\text{K}^{\Delta})\,(k_{et}^{\Lambda}/k_{et}^{\Delta}) \qquad (14)$$

For the system Tb(dpa)$_3^{3-}$/**1**, we have $E_q = -0.24$, $E_b = -0.7$, and, hence, $k_q^{\Lambda}/k_q^{\Delta} = 1.6$, $K'^{\Lambda}/K^{\Delta} = 6$. Using eq 14, one then calculates $(k_{et}^{\Lambda}/k_{et}^{\Delta}) = 0.3$; for Eu, one finds virtually the same number. This result implies that the enantioselectivity in the binding of the lanthanide chelates to the quencher is counteracted by a selectivity of opposite sign in the energy transfer step within the encounter complexes. The chiral discrimination in the binding is stronger than the selectivity in the energy transfer process so that, with the corrinoids, the overall chirality dependence of the quenching rates reflects the selectivity in the complexation.

A second point to discuss is the difference of the E_q values for Tb and Eu with the same quencher (cf Tables 1 and 2). Replacing Tb by Eu will leave the steric and electrostatic interactions between the reaction partners largely unaltered and thus not affect the enantioselectivity in the binding drastically. In contrast, k_{et}, which contains the matrix element, $\langle\Psi(\text{Ln* Q})|H|\Psi(\text{Ln Q*})\rangle$, may change because the wave functions of Tb* and Eu* differ, and therefore the enantioselectivity in the energy transfer step.

For many quenchers in Tables 2 and 3, the values of E_q for $Tb(dpa)_3^{3-}$ and $Eu(dpa)_3^{3-}$ differ by <20%. In the same fashion, quenching of Tb and $Dy(dpa)_3^{3-}$ by $Ru(phen)_3^{2+}$ occurs with very similar selectivities.[16] Also, for the quenching by cobalt hexamine chelates, relatively small, but significant, differences in E_q were observed for Tb and Eu.[8] The fact that similar E_q values are observed indicates that the ratios $k_{et}^{\Delta}/k_{et}^{\Lambda}$ must be very similar for various $Ln(dpa)_3^{3-}$ species. Assuming that the differences between k_{et}^{Δ} and k_{et}^{Λ} are brought about by differences in the distance and relative orientation of the donor and acceptor in the two diastereomeric encounter complexes, it follows that this geometry dependence of the energy transfer rate k_{et} must be essentially the same for the lanthanide ions in order to produce almost equal E_q values.[16] Such a situation is expected if, for instance, a similar dipole−dipole interaction would be the dominating term in the multipole expansion of the matrix elements $\langle\Psi(\text{Tb* Q})|\text{H}|\Psi(\text{Tb Q*})\rangle$ and $\langle\Psi(\text{Eu* Q})|\text{H}|\Psi(\text{Eu Q*})\rangle$.

There is a second mechanism which can give rise to discrepant E_q values for Tb and Eu. In general, the quenching rates for Eu and Tb are different, and this allows for the possibility that for the luminophore which is quenched faster, the energy transfer reaction is more strongly controlled by diffusion processes. As mentioned, (partial) diffusion control would result in a lowering of the $|E_q|$ value. So even when the intrinsic selectivity is the same for both Tb and Eu, this might account for a discrepancy between the E_q values. For the cytc proteins, however, the observation that the selectivity for both Eu and Tb is independent of ionic strength provides an indication that the variation of E_q is due to a difference in energy transfer mechanism;[25] the mutual diffusion rates of charged species are known to depend on ionic strength, and therefore, if the energy transfer reaction is under partial diffusion control, the selectivity is expected to vary with ionic strength, as was experimentally observed for $Tb(dpa)_3^{3-}$ and $Ru(phen)_3^{2+}$ in methanol.[14]

This brings us again to the question whether a variation of the energy transfer mechanism is feasible upon changing the central lanthanide ion. An average value of the energy transfer rates k_{et}^{Δ} and k_{et}^{Δ} may be calculated from the experimental quenching rates and binding constant using eq 8. One obtains $k_{et}^{avg} = 3 \times 10^7$, 1×10^7, and 5×10^8 s^{-1} for energy transfer from Tb to **1**, **2**, and **4**, respectively. For Eu, the corresponding values are 1×10^6, 4×10^7, and 1×10^8 s^{-1} (for the charged species **2**, the effect of ionic strength on the quenching rate has been taken into account).[28]

For quenchers with allowed optical transitions in the wavelength region of the lanthanide emission bands, Stryer, Meares, and co-workers[56] have used Förster theory[57] to calculate energy transfer rates. Using a similar approach, we calculate for the case of Tb $k_{et} = 0.9$, 0.7, and 1.2×10^7 s^{-1} for **1**, **2**, and **4**, respectively, and, for Eu, 0.16, 0.36, and 1.3×10^6 s^{-1}.[58] In all cases, the Förster-type approach predicts smaller rates than those determined from experiment, and the differences range from a factor of ~1 up to a factor of 10^2. Apparently, the calculated rates are not proportional to the "spectral overlap" between the luminescence of the donor and the absorption of the acceptor (spectra shown in Figure 3). Thus, they are not in keeping with a simple Förster model for the energy transfer—at least not in all donor−acceptor systems. It might well be that mechanisms other than the dipole−dipole coupling, e.g., higher multipole−multipole and/or exchange interactions, are also operative and could, in certain cases, even be stronger than the Förster-type interaction. It should be pointed out that for cobalt hexamine[10] and cobalt EDTA chelates,[56] which are very efficient quenchers of $Tb(dpa)_3^{3-}$ and $Eu(dpa)_3^{3-}$ luminescence, it is unlikely that energy transfer proceeds via the Förster dipole−dipole mechanism because the lanthanide emission bands overlap mainly with dipole forbidden transitions of the cobalt complexes. For these quenchers, an exchange or Dexter type quenching mechanism was proposed.

Probing Binding of Vitamin B_{12} to Proteins by Enantioselective Quenching

The experiments described above show that B_{12} is a rather effective quencher of $Tb(dpa)_3^{3-}$ luminescence and that it has a specific binding site for the lanthanide chelate involving the a and g side chains of the corrin ring. These observations led us to the idea that the energy transfer reactions might be used to probe the binding of B_{12} to proteins. If, for instance, the B_{12} species were to be encapsulated by a protein, then the selectivity and rate of the lanthanide luminescence quenching would to a large extent be determined by the outer surface of the protein surrounding the B_{12}. In this case, one expects the enantioselectivity to change significantly upon addition of B_{12}-binding protein to the $B_{12}-Tb(dpa)_3^{3-}$ solution.

To test this idea, we have measured the effect of two B_{12}-binding proteins on the rate and enantioselectivity of the luminescence quenching of $Tb(dpa)_3^{3-}$ by B_{12}: a monoclonal antibody and haptocorrin.[29] The results are illustrated in Figure 9. Addition of the antibody to a solution of Ln and B_{12} results in an acceleration of the quenching and a change in the enantioselectivity. In the titration curve, an inflection point occurs when the mole ratio of B_{12} to antibody is ~2:1, consistent with the presence of two identical binding sites for B_{12} on Igg type antibodies.[59] The higher quenching rate for the B_{12} antibody adduct could, by measurement of the ionic strength dependence of the rates, be ascribed to attractive electrostatic interactions between positively charged amino acid residues near the B_{12} binding site and the negatively charged Ln chelate. The B_{12} alone has no net charge. The higher quenching rate for the adduct implies that the B_{12} is still accessible for negatively charged ions in solution when bound to the protein. The change in enantioselectivity implies that the binding site for $Tb(dpa)_3^{3-}$ on B_{12} made up by the a and g side chains is blocked by complexation to the antibody. In contrast, binding of B_{12} to haptocorrin results in a strong decrease of the quenching rate. In this case, an inflection point occurs at equimolar quantities of B_{12} and protein, consistent with binding of one B_{12} per haptocorrin. For haptocorrin concentrations such that there is still a measurable quenching, the enantioselectivity has not changed with respect to the selectivity observed of the free B_{12}. This is consistent with the idea that the remaining free B_{12} is the main quencher in solution.

Summary and Outlook

With the advent of time-resolved circular polarization measurements of lanthanide luminescence, accurate and detailed studies of chiral discrimination in energy transfer reactions in aqueous solution have become possible. For the system Ln-

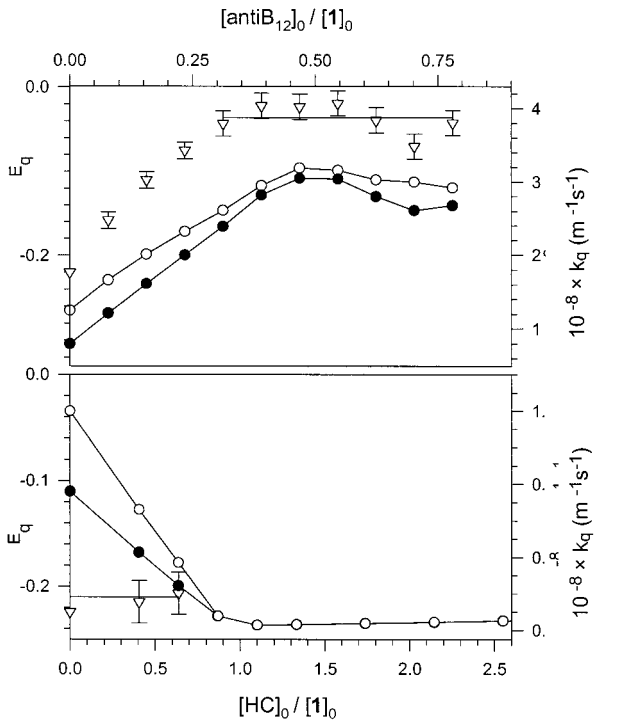

Figure 9. Effect of anti-B_{12} antibody on the quenching of $Tb(dpa)_3^{3-}$ luminescence by **1** (upper graph). Effect of haptocorrin (HC) on the quenching (lower graph). Values of E_q (triangles, vertical bars denote the standard error), k_q^{Λ} (open circles), and k_q^{Δ} (filled circles) are plotted against the ratio of the total concentrations of **1** and protein. Sample conditions: $[Tb(dpa)_3^{3-}]$= 0.2 mM, 10 mM Hepes buffer, pH 7.2, and [**1**] = 3 μM and 9 μM for the upper and lower graph, respectively.

$(dpa)_3^{3-}/B_{12}$, it could be shown that the enantioselectivity observed in the transfer results to a large extent from enantiodifferential stability of the encounter complexes of photoexcited donor and acceptor. The existence of such encounter complexes, for which the negative activation energies of the quenching reaction give already a strong indication, could be substantiated by NMR and CD measurements. The general picture which emerges is that the lanthanide chelate and the B_{12} species in water form a complex with a binding enthalpy of ~kJ/mol. Among the intermolecular forces contributing to the stability of the encounter complex, hydrogen-bonding interactions between the carboxylate groups of the dpa ligand and the amide protons of the a and g side chains of the corrin ring play an important role. As yet, the nature of the electronic interactions which are responsible for the energy transfer step remain elusive. It seems likely that dipole−dipole interactions alone cannot account for the interaction. Even though many details of the intriguing quantum mechanical energy transfer are not fully understood, the quenching reactions can be used to probe structural aspects of complex (bio)molecules and to monitor the accessibility of metals centers in large molecules to the luminescent ions in solution. This was illustrated with a few examples involving B_{12} derivatives and c-type cytochromes. An interesting future application of the enantioselective luminescence technique may be the study of metal containing membrane proteins.

References and Notes

(1) Kaizu, Y.; Mori, T.; Kobayashi, H. *J. Phys. Chem.* **1985**, *89*, 332.

(2) Metcalf, D. H.; Snyder, S. W.; Wu, S.; Hilmes, G. L.; Riehl, J. P.; Richardson, F. S. *J. Am. Chem. Soc.* **1989**, *111*, 3082.

(3) Metcalf, D. H.; Snyder, S. W.; Demas, J. N.; Richardson F. S. *J. Phys. Chem.* **1990**, *94*, 7143.

(4) Metcalf, D. H.; Snyder, S. W.; Demas, J. N.; Richardson F. S. *Eur. J. Solid State Inorg.* **1991**, *28*, 57.

(5) Richardson, F. S.; Metcalf, D. H.; Glover, D. P. *J. Phys. Chem.* **1991**, *95*, 6249.

(6) Glover, D. P.; Metcalf, D. H.; Richardson F. S. *J. Alloys Compd.* **1992**, *180*, 83.

(7) Metcalf, D. H.; Bolender, J. P.; Driver, M. S.; Richardson, F. S. *J. Phys. Chem.* **1993**, *97*, 553.

(8) Bolender, J. P.; Metcalf, D. H.; Richardson, F. S. *Chem. Phys. Lett.* **1993**, *213*, 131.

(9) Bolender, J. P.; Metcalf, D. H.; Richardson, F. S. *J. Alloys Compd.* **1994**, *207−208*, 55.

(10) Glover-Fischer, D. P.; Metcalf, D. H.; Bolender, J. P.; Richardson, F. S. *Chem. Phys.* **1995**, *198*, 207.

(11) Chisdes, S. J.; Richardson F. S. *Abstr. Pap. Am. Chem. Soc.* **1997**, *213*, 110.

(12) Wu, S. G.; Bedard, T. C.; Riehl, J. P. *Collect. Czech. Chem. Commun.* **1991**, *56*, 3025.

(13) Rexwinkel, R. B.; Meskers, S. C. J.; Riehl, J. P.; Dekkers, H. P. J. M. *J. Phys. Chem.* **1992**, *96*, 1112.

(14) Rexwinkel, R. B.; Meskers, S. C. J.; Dekkers, H. P. J. M.; Riehl, J. P. *J. Phys. Chem.* **1992**, *96*, 5725.

(15) Rexwinkel, R. B.; Meskers, S. C. J.; Riehl, J. P.; Dekkers, H. P. J. M. *J. Phys. Chem.* **1993**, *97*, 3875.

(16) Rexwinkel, R. B.; Meskers, S. C. J.; Dekkers, H. P. J. M.; Riehl, J. P. *J. Phys. Chem.* **1993**, *97*, 13519.

(17) Maupin, C. L.; Meskers, S. C. J.; Dekkers, H. P. J. M.; Riehl, J. P. *Chem. Commun.* **1996**, 2457−2458.

(18) Maupin, C. L.; Meskers, S. C. J.; Dekkers, H. P. J. M.; Riehl, J. P. *J. Phys. Chem.* A **1998**, *102*, 4450.

(19) Meskers, S. C. J.; Dekkers, H. P. J. M. *J. Alloys Compds.* **1997**, *250*, 332.

(20) Meskers, S. C. J.; Dekkers, H. P. J. M.; Rapenne, G.; Sauvage, J.-P. *Chem. Eur. J.* **2000**, *6*, 2129.

(21) Metcalf, D. H.; Stewart, J. M. McD.; Snyder, S. W.; Grisham, C. M.; Richardson, F. S. *Inorg. Chem.* **1992**, *31*, 2445.

(22) Stockman, T. G.; Klevickis, C. A.; Grisham, C. M.; Richardson, F. S. *J. Mol. Recognit.* **1996**, *9*, 595.

(23) Meskers, S. C. J.; Ubbink, M.; Canters; G. W.; Dekkers, H. P. J. M. *J. Phys. Chem.* **1996**, *100*, 17957.

(24) Meskers, S. C. J.; Dekkers, H. P. J. M. *Enantiomer* **1998**, *3*, 95.

(25) Meskers, S. C. J.; Ubbink, M.; Canters, G. W.; Dekkers, H. P. J. M. *J. Biol. Inorg. Chem.* **1998**, *3*, 463.

(26) Meskers, S. C. J.; Dennison, C.; Canters, G. W.; Dekkers, H. P. J. M. *J. Biol. Inorg. Chem.* **1998**, *3*, 663.

(27) Meskers, S. C. J.; Dekkers, H. P. J. M. Unpublished results.

(28) Meskers, S. C. J.; Dekkers, H. P. J. M. *Spectrochim. Acta A* **1999**, *55*, 1857.

(29) Meskers, S. C. J.; Dekkers, H. P. J. M. *J. Am. Chem. Soc.* **1998**, *120*, 6413.

(30) (a) Brittain, H. G. *Chirality* **1996**, *8*, 357. (b) Riehl, J. P. *Acta Phys. Pol., A* **1996**, *90*, 55. (c) Dekkers, H. P. J. M. In *Circular Dichroism, Principles and Applications*; Berova, N., Nakanishi, K., Woody, R. W., Eds.; Wiley-VCH Publishers: New York, 2000. (d) Riehl, J. P.; Richardson, F. S. *Method Enzymol.* **1993**, *226*, 539−553. (e) Richardson, F. S. *J. Less-Common Met.* **1989**, *149*, 161−177. (f) Brittain, H. G. *J. Coord. Chem.* **1989**, *20*, 331. (g) Brittain, H. G. *Photochem. Photobiol.* **1987**, *46*, 1027. (h) Riehl, J. P.; Richardson, F. S. *Chem. Rev.* **1986**, *86*, 1. (i) Richardson, F. S.; Riehl, J. P. *Chem. Rev.* **1977**, *77*, 773.

(31) Rexwinkel, R. B.; Schakel, P.; Meskers, S. C. J.; Dekkers, H. P. J. M. *Appl. Spectrosc.* **1993**, *47*, 731.

(32) Kemp, J. C. *J. Opt. Sci. Am.* **1969**, *59*, 950.

(33) (a) Albertsson, J. *Acta Chem. Scand.* **1970**, *24*, 1213. (b) Albertsson, J. *Acta Chem. Scand.* **1972**, *26*, 985. (c) Albertsson, J. *Acta Chem. Scand.* **1972**, *26*, 1005. (d) Albertsson, J. *Acta Chem. Scand.* **1972**, *26*, 1023. (e) Shengzhi, H.; Zhenchao, D.; Huizhen, Z.; Qiwang, L. *Xiamen Daxue Xuebao, Ziran Kexueban* **1989**, *28*, 58. (f) *Shengzhi, H.; Zhenchao, D.; Huizhen, Z.; Qiwang, L. Xiamen Daxue Xuebao, Ziran Kexueban* **1989**, *28*, 279. (g) *Shengzhi, H.; Zhenchao, D.; Huizhen, Z.; Qiwang, L. Xiamen Daxue Xuebao, Ziran Kexueban* **1989**, *28*, 514. (h) Brayshaw, P. A.; Harrowfield; J. M. *Acta Crystallogr.* **1995**, *C51*, 1799. (i) VanMeervelt, L.; Binnemans, K.; VanHerck, K.; GorllerWalrand, C. *Bull. Soc. Chim Belges* **1997**, *106*, 25.

(34) Meskers, S. C. J.; Riehl, J. P.; Dekkers, H. P. J. M. *Chem. Phys. Lett.* **1993**, *216*, 241.

(35) (a) Metcalf, D. H.; Snyder, S. W.; Demas, J. N.; Richardson, F. S. *J. Am. Chem. Soc.* **1990**, *112*, 469. (b) Metcalf, D. H.; Snyder, S. W.; Demas, J. N.; Richardson F. S. *Eur. J. Solid State Inorg.* **1991**, *28*, 65−68; 255. (c) Glover-Fischer, D. P.; Metcalf, D. H.; Hopkins, T. A.; Pugh, V. J.; Chisdes, S. J.; Kankare, J.; Richardson, F. S. *Inorg. Chem.* **1998**, *37*, 3026.

(36) Sherry, A. D.; Geraldes, C. F. G. C. In *Lanthanide probes in Life, Chemical and Earth Sciences*; Bünzli, J.-C. G., Choppin, G. R., Eds.; Elsevier: Amsterdam, 1989; Chapter 4.

(37) Northrup, S. H.; Wensel, T. G.; Meares, C. F.; Wendolski, J. J.; Matthews, J. B. *Proc. Natl. Acad. Sci. U.S.A.* **1990**, *87*, 9503.

(38) Moore, G. W.; Pettigrew, G. R. *Cytochromes c. Evolutionairy, Structural and Physiochemical aspects*; Springer-Verlag: Berlin, 1990.

(39) Benning, M. M.; Meyer, T. E.; Holden, H. M. *Arch. Biochem. Biophys.* **1994**, *310*, 460.

(40) Timkovich, R.; Dickerson, R. E. *J. Biol. Chem.***1976**, *251*, 4033.

(41) The older name for this organism is *Thiobacillus versutus*. Katayama, Y.; Hiraishi, A.; Kuraishi, H. *Microbiology* **1995**, *141*, 1469.

(42) (a) Ubbink, M.; Van Beeumen, J.; Canters, G. W. *J. Bacteriol.* **1992**, *174*, 3707. (b) Ubbink, M.; Canters, G. W. *Biochemistry* **1993**, *32*, 13893. (c) Ubbink, M.; Campos, A. P.; Teixeira, M.; Hunt, N. I.; Hill, H. A. O.; Canters, G. W. *Biochemistry* **1994**, *33*, 10051. (d) Ubbink, M.; Hunt, N. I.; Hill, H. A. O.; Canters, G. W. *Eur. J. Biochem.* **1994**, *222*, 561. (e) Ubbink, M.; Warmerdam, G. C. M.; Campos, A. P.; Teixeira, M.; Canters, G. W. *FEBS Lett.* **1994**, *351*, 100.

(43) Meskers, S. C. J.; Dekkers, H. P. J. M. Unpublished results.

(44) Narimatsu, S.; Kato, R.; Horie, T.; Ono, S.; Tsutsui, M.; Yabusaki, Y.; Ohmori, S,; Kitada, M.; Ichioka, T.; Shimada, N.; Kato, R.; Ishikawa, T. *Chirality* **1999**, *11*, 1.

(45) Ellis, S. W.; Hayhurst, G. P.; Lightfoot, T.; Smith, G.; Harlow, J.; Rowland-Yeo, K.; Larsson, C.; Mahling, J.; Lim, C. K.; Wolf, C. R.; Blackburn, M. G.; Lennard, M. S.; Tucker, G. T. *Biochem. J.* **2000**, *345*, 565.

(46) Narimatsu, S.; Kobayashi, N.; Masubuchi, Y.; Horie, T.; Kakegawa, T.; Kobayashi, H.; Hardwick, J. P.; Gonzalez, F. J.; Shimada, N.; Ohmori, S.; Kitada, M.; Asaoka, K.; Kataoka, H.; Yamamoto, S.; Satoh, T. *Chem.-Biol. Interact.* **2000**, *127*, 73.

(47) Meskers, S. C. J.; Dekkers, H. P. J. M. Spectrochimica Acta A **1999**, *55*, 1837.

(48) (a) Pratt, J. M. *Inorganic Chemistry of Vitamin B_{12}*; Academic Press: London, 1972. (b) Giannotti, C. In *B_{12}*; Dolphin, D., Ed.; Wiley: New York, 1982; Vol. I, pp 393−431. (c) Toraya, T.; Fukui, S. Metalloproteins. In *Bioactive Molecules*; Oisuka, S., Yamanaka, T., Eds.; Elsevier: New York, 1988; Vol. 8.

(49) (a) Eilbeck, W. J.; West, M. S.; Owen, Y. E. *J. Chem. Soc., Dalton Trans.* **1972**, 2205. (b) Brown, K. L.; Cheng, S., Zou, X.; Zubkowski, E. J.; Valente, E. J.; Knapton, L.; Marques, H. M. *Inorg. Chem.* **1997**, *36*, 3666.

(50) Hart, F. A. *Comprehensive Coordination Chemistry*; Wilkinson, G., Ed.; Pergamon Press: Oxford UK, 1987; Vol. 3, Chapter 39.

(51) Bertini, I.; Luchinat, C. *Coord. Chem. Rev.* **1996**, *150*.

(52) Dwek, R. A. *Nuclear Magnetic Resonance in Biochemistry*; Clarendon Press: Oxford, 1973.

(53) Desreux, J. F.; Reilley, C. N. *J. Am. Chem. Soc.* **1976**, *98*, 2105.

(54) (a) Zitha-Bovens, E.; van Bekkum, H.; Peters, J. A.; Geraldes, C. F. G. C. *Eur. J. Inorg. Chem.* **1999**, *2*, 287. (b) Carvalho, R. A.; Peters, J. A.; Geraldes, C. F. G. C. *Inorg. Chim. Acta* **1997**, *262*, 167.

(55) Huskowska, E.; Riehl, J. P. *Inorg. Chem.* **1995**, *34*, 5615.

(56) (a) Stryer, L.; Thomas, D. D.; Meares, C. F. *Annu. Rev. Biophys. Bioeng.* **1982**, *11*, 203. (b) Meares, C. F.; Yeh, S. M.; Stryer, L. *J. Am. Chem. Soc.* **1981**, *103*, 1607. (c) Meares, C. F.; Wensel, T. G. *Acc. Chem. Res.* **1984**, *17*, 202.

(57) See, e.g.: Speiser, S. *Chem. Rev.* **1996**, *96*, 1953.

(58) A 9 Å distance between the Ln and Co atoms (as determined from NMR measurements) was used in the calculation, and the spectral overlap between lanthanide emission and corrinoid absorption spectra was determined. For $Eu(dpa)_3^{3-}$, the magnetic dipole transition at 595 nm has been neglected in the determination of the spectral overlap. In the calculation, the following numbers were used: decay rate and quantum yield for luminescence for $Tb(dpa)_3^{3-}$, $k_0 = 472\ s^{-1}$, $\phi_{lum} = 0.7$; for $Eu(dpa)_3^{3-}$, $k_0 = 622\ s^{-1}$, $\phi_{lum} = 0.3$. Orientation factor $\kappa^2 = 1$ (for dipoles parallel to each other and perpendicular to the line connecting them).

(59) See, e.g.: Alberts, B.; Bray, D.; Lewis, J.; Raff, M.; Roberts, K.; Watson, J. D. *Molecular Biology of the Cell*; Garland Publishing: New York, 1994.